



The significance of model structure in one-dimensional stream solute transport models with multiple transient storage zones – competing vs. nested arrangements



P.C. Kerr^{a,*}, M.N. Gooseff^{b,1}, D. Bolster^a

^a Department of Civil and Environmental Engineering and Earth Sciences, University of Notre Dame, IN, United States

^b Department of Civil and Environmental Engineering, The Pennsylvania State University, PA, United States

ARTICLE INFO

Article history:

Received 6 December 2012

Received in revised form 3 May 2013

Accepted 5 May 2013

Available online 1 June 2013

This manuscript was handled by Peter K. Kitanidis, Editor-in-Chief, with the assistance of Philippe Négrel, Associate Editor

Keywords:

Transport

Hyporheic

Transient storage

Solute

Streams

Tracer

SUMMARY

Transient storage models are commonly used to simulate solute transport in streams to characterize hydrologic controls on biogeochemical cycling. Recently, 2-storage zone (2-SZ) models have been developed to represent in-channel surface transient storage (STS) and hyporheic transient storage (HTS) separately to overcome the limitations of single storage zone (1-SZ) models. To advance biogeochemical models, we seek to separate the effects of these storage zones on solute fate and cycling in streams. Here we compare and contrast the application and interpretations from two model structures that include STS and HTS storage: a *competing* model structure, where both zones are connected to the stream at the same location and the stream interacts with the STS and HTS separately, and a *nested* model structure, where STS is an intermediary between the stream and HTS. We adapt common residence time metrics used to compare single transient storage models for the competing and nested 2-SZ models. As a test case, we investigated the transient storage characteristics of a first-order stream in Pennsylvania, using 1-SZ, nested 2-SZ, and competing 2-SZ model configurations at several different flow conditions. While both 2-SZ models fit the observed STS and in-stream breakthrough curves well, calibrated model parameters and solute molecule travel paths differ, as evident by the faster exchange rate displayed by the nested model, and therefore so does the interpretation of associated transient storage metrics and its relationship with biogeochemical cycling processes. In addition, a study of hypothetical zone-specific reaction rates was very illustrative of the differences in discrimination characterized by each model structure, particularly for the case where reactions would predominantly occur in the STS (i.e. photochemical reactions), because of the compounding effects to the HTS for the nested 2-SZ; however, for the case where reactions would predominantly occur in the HTS, the influence of model structure was found to be relegated only to the HTS.

© 2013 Published by Elsevier B.V.

1. Introduction

Low-order streams are at the head of the river continuum and are the primary interface between the river network and its drainage basin (Vannote et al., 1980). These streams feature a strong connectivity with the riparian ecosystem due to channel complexity and stream gradient, resulting in hydraulic characteristics and biogeochemical conditions that differ from high-order streams (Anderson et al., 2005). Studies addressing the simulation of hydrodynamic and biogeochemical processing of these streams have led

to the development of conceptual models that approximate complex geometry and physics by incorporating transient storage, a process of mass exchange with a non-advective region that simulates the skew of breakthrough curves from tracer experiments (Hays et al., 1966; Thackston and Krenkel, 1967; Thackston and Schnelle, 1970). These models provide insight into areas of the stream difficult to observe and their interpretation are facilitated by metrics to quantify biogeochemical and hydraulic characteristics at the local, reach, or watershed scales. Similar models have also had great success in other branches of hydrology such as groundwater systems (Haggerty and Gorelick, 1995).

Bencala and Walters (1983) describe transient storage as stagnant or slow relative to the longitudinal flow of the stream; this might include locations such as edges of pools, backwaters, and subsurface exchange of water. This definition of transient storage serves as the foundation for current single transient storage models (1-SZ) for one-dimensional solute transport, where transient

* Corresponding author. Address: Department of Civil and Environmental Engineering and Earth Sciences, University of Notre Dame, 156 Fitzpatrick Hall, Notre Dame, IN 46556, United States. Tel.: +1 574 631 3864; fax: +1 574 631 9236.

E-mail address: PCorbettKerr@gmail.com (P.C. Kerr).

¹ Present address: Department of Civil and Environmental Engineering, Colorado State University, Fort Collins, CO 80523-1372, United States.

storage is considered to be a bulk storage zone with no discrimination in the model between potentially very different types of storage zones such as surface transient storage (STS; slack-water in the channel) and hyporheic transient storage (HTS; exchange of stream water through the subsurface). It is most typically represented mathematically as a single-order mass transfer process. Originally coined “dead zone models”, solute transport models that accommodate transient storage have been studied under a variety of nomenclatures, from theoretical, to laboratory to field (Bencala and Walters, 1983). They were created and applied to account for solute transport that is not well described by the advection–dispersion equation alone. While single storage zone models are effective for simulating solute transport, they fail to discriminate the processes within each of the disparate storage zones – surface vs. subsurface (Choi et al., 2000; Gooseff et al., 2005; Harvey et al., 1996). Recent research has focused on two-storage zone (2-SZ) models that discriminate STS and HTS (Briggs et al., 2009; Briggs et al., 2010; Marion et al., 2008; Choi et al., 2000; Bottacin-Busolin et al., 2011). In principle though as many storage zones as desired or needed can be incorporated (Haggerty and Gorelick, 1995), depending on the processes to be modeled, and information available to constrain characterization of the model domains.

STS and HTS are subject to different biogeochemical conditions (Runkel et al., 2003). Surface water can receive sunlight and oxy-

gen and has bed contact along its perimeter, while subsurface water does not receive sunlight, may be anoxic, and is sated by porous media (Briggs et al., 2009). Not all STS are restricted to eddies or the edge of water as vegetation or boulders (in the case of gravel bed rivers) can also provide a thick boundary layer of extremely slow moving water along the bed of the main channel (MC) that can also act as STS and can have unique biogeochemical properties (Harvey et al., 2005). Models that account for multiple storage zones have the ability to discriminate the transport processes within these zones and thus potentially biogeochemical processes also (Donado et al., 2009; Willmann et al., 2010).

Biogeochemical processing is dependent on hydrodynamic transport factors such as residence time, travel path, and flowpath conditions (Zarnetske et al., 2011), which when simulated by a multiple transient storage zone model can be sensitive to the zonal interaction described by the structure of the model (Stewart et al., 2011). In multiple transient storage zone models, each storage zone can interact with the stream, another storage zone, or both. Current 2-SZ models have a competing storage model structure in which the exchange between each storage zone occurs directly with the main channel (i.e., water or solute entering storage goes into one storage zone or the other), but not with each other (Fig. 1). We propose an alternative nested 2-SZ model structure in which the storage zones interact by nesting the STS zone between the stream and

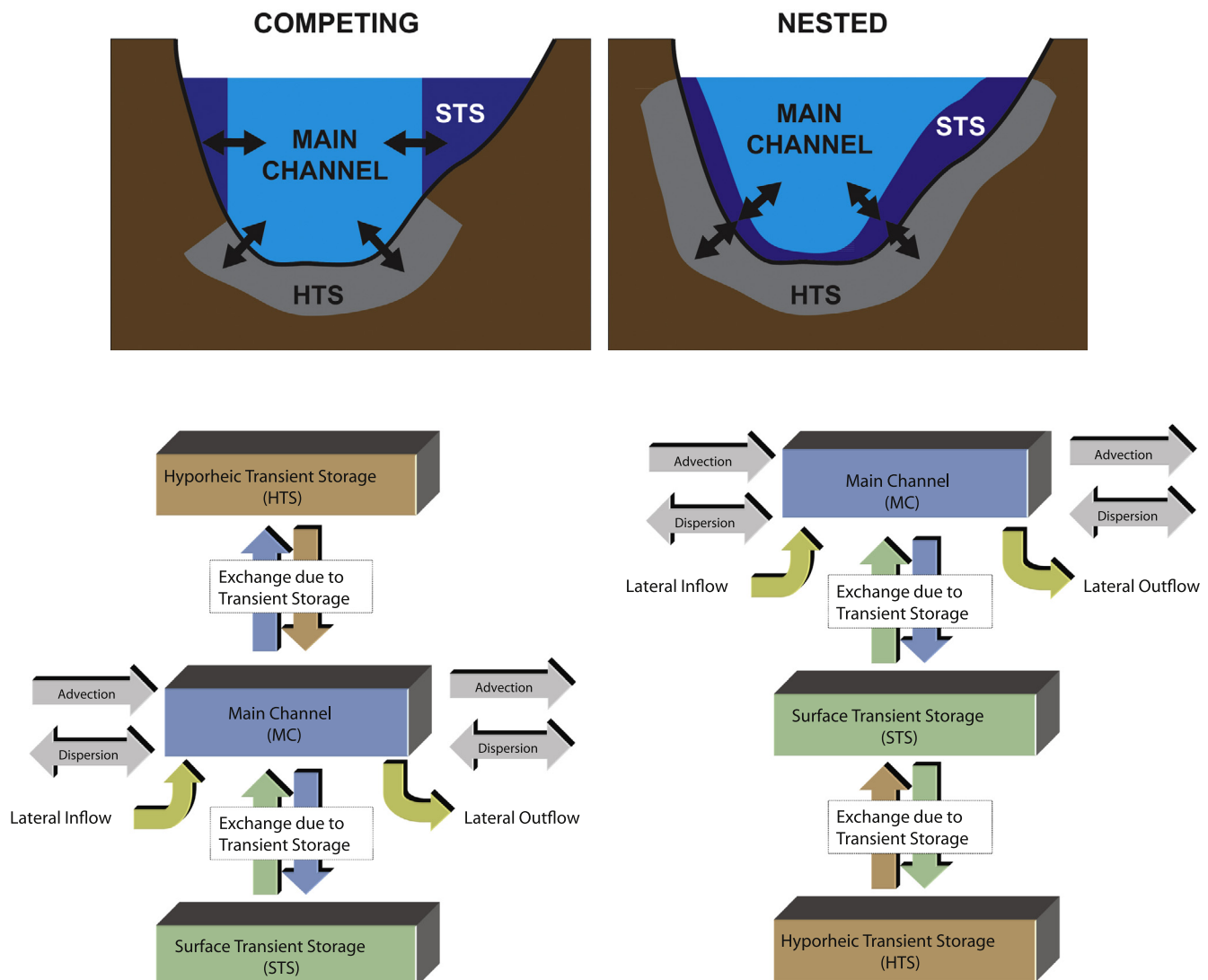


Fig. 1. An example of conceptual layouts of C2-SZ and N2-SZ Model structures.

the HTS zone. The structure of the transient storage model determines the process and path by which solute molecules pass through storage zones and for how long they remain within individual parts of the system. This study examines the implications of three potential model structures, 1-SZ, competing 2-SZ, and nested 2-SZ by investigating the transient storage characteristics of a first-order Pennsylvania stream and comparing the calibrated model parameters, analytical metrics, and physical interpretations.

2. Model

2.1. Model structure

The two primary processes that determine the solute concentration from stream tracer experiments are hydrologic transport and chemical transformation (Runkel, 2002). For a conservative or reactive tracer, the single transient storage zone (1-SZ) model is commonly described by the following coupled differential equations:

$$\frac{\partial C}{\partial t} = -\frac{Q}{A} \frac{\partial C}{\partial x} + \frac{1}{A} \frac{\partial}{\partial x} \left(AD \frac{\partial C}{\partial x} \right) + \frac{q_L}{A} (C_L - C) + \alpha (C_S - C) - \lambda C \quad (1)$$

$$\frac{dC_S}{dt} = \alpha \frac{A}{A_S} (C - C_S) - \lambda_S C_S \quad (2)$$

where A is the main channel cross-sectional area (L^2), A_S the storage zone cross-sectional area (L^2), C the main channel solute concentration (M/L^3), C_S the storage zone solute concentration (M/L^3), D the dispersion coefficient (L^2/T), Q the volumetric flow rate (L^3/T), q_L the lateral inflow rate (L^3/T), C_L the lateral inflow concentration (M/L^3), λ the main channel first-order decay coefficient (T^{-1}), λ_S the storage zone first-order decay coefficient (T^{-1}), α is the storage zone exchange coefficient ($1/T$)

The current most widely accepted model structure for a two-storage zone model that discriminates between the STS and HTS is the competing transient storage zone (C2-SZ) model, where a second transient storage zone is added to the 1-SZ model in parallel fashion (Choi et al., 2000; Gooseff et al., 2004; Briggs et al., 2009). In the C2-SZ model, the additional storage zone interacts only with the main channel and not the other storage zone (see Fig. 1).

$$\frac{\partial C}{\partial t} = -\frac{Q}{A} \frac{\partial C}{\partial x} + \frac{1}{A} \frac{\partial}{\partial x} \left(AD \frac{\partial C}{\partial x} \right) + \frac{q_L}{A} (C_L - C) + \alpha_{STS} (C_{STS} - C) + \alpha_{HTS,C} (C_{HTS} - C) - \lambda C \quad (3)$$

$$\frac{dC_{STS}}{dt} = \alpha_{STS} \frac{A}{A_{STS}} (C - C_{STS}) - \lambda_{STS} C_{STS} \quad (4)$$

$$\frac{dC_{HTS}}{dt} = \alpha_{HTS,C} \frac{A}{A_{HTS}} (C - C_{HTS}) - \lambda_{HTS} C_{HTS} \quad (5)$$

where A_{STS} is the STS cross-sectional area (L^2), A_{HTS} the HTS cross-sectional area (L^2), C_{STS} the STS solute concentration (M/L^3), C_{HTS} the HTS solute concentration (M/L^3), λ_{STS} the STS first-order decay coefficient (T^{-1}), λ_{HTS} the HTS first-order decay coefficient (T^{-1}), α_{STS} the STS exchange coefficient (T^{-1}), $\alpha_{HTS,C}$ is the C2-SZ HTS exchange coefficient (T^{-1}).

An alternative to the C2-SZ model structure, termed the nested transient storage zone (N2-SZ) model is proposed, where a second transient storage zone is added to the 1-SZ model in serial fashion. In the N2-SZ model, the additional storage zone interacts only with the other storage zone and not the main channel (see Fig. 1).

$$\frac{\partial C}{\partial t} = -\frac{Q}{A} \frac{\partial C}{\partial x} + \frac{1}{A} \frac{\partial}{\partial x} \left(AD \frac{\partial C}{\partial x} \right) + \frac{q_L}{A} (C_L - C) + \alpha_{STS} (C_{STS} - C) - \lambda C \quad (6)$$

$$\frac{dC_{STS}}{dt} = \alpha_{STS} \frac{A}{A_{STS}} (C - C_{STS}) + \alpha_{HTS,N} (C_{HTS} - C_{STS}) - \lambda_{STS} C_{STS} \quad (7)$$

$$\frac{dC_{HTS}}{dt} = \alpha_{HTS,N} \frac{A_{STS}}{A_{HTS}} (C_{STS} - C_{HTS}) - \lambda_{HTS} C_{HTS} \quad (8)$$

where $\alpha_{HTS,N}$ is the N2-SZ HTS exchange coefficient (T^{-1}).

The three potential model structures, 1-SZ, C2-SZ, and N2-SZ, conceptualize a stream system where:

- (1) Storage is characterized by a well-mixed non-advective zone.
- (2) The main channel is characterized by one-dimensional advection–dispersion.
- (3) Mass exchange has a first order relationship described by an exchange coefficient and the difference in concentration between zones.
- (4) Some of the model parameters are physically measurable (e.g., A , A_{STS}).

The 2-SZ models replace the storage zone parameters from the 1-SZ model with parameters that self-describe the type of storage zone involved (i.e. STS or HTS). Many of the C2-SZ model parameters have the same physical definition as the N2-SZ model parameters, so no identification was made to differentiate the names between the model structures, aside from α_{HTS} denoted by $(_N)$ for the N2-SZ model (i.e. $\alpha_{HTS,N}$) and $(_C)$ for the C2-SZ model (i.e. $\alpha_{HTS,C}$). In the C2-SZ model, the α_{HTS} characterizes the exchange between the HTS and MC, whereas in the N2-SZ, it describes the exchange between the HTS and STS.

2.2. Physical interpretation of model structures

The competing and nested model structures represent two potential extremes of conceptual interactions between storage zones and the main channel. Each model structure presented in this study is a simplified interpretation of the natural system's complex physics. In a natural system the STS and HTS have advective transport components, whereas a major assumption of the transient storage model is that the storage zones are non-advective. As shown in Fig. 1, the C2-SZ model structure prevents exchange of solute between the stream and HTS in areas where the STS does not exist, so that exchange between the HTS and MC occurs in patches. By contrast, in the N2-SZ model structure solute exchanges with the HTS in places where the STS exists, as part of a uniform layered system. A common feature of flow structure in rivers and streams is the tree-ring downstream velocity profile and the lower advection along the bed's boundary layer, which is what the nested model structure conceptualizes. We envision that the natural system is a mix of both of these types of model structures, because exchange with the HTS and STS is likely neither entirely layered nor entirely separate, but rather a combination of these two conceptual descriptions of the physical environment.

This conceptualization of a single STS and a single HTS is not a complete or conclusive discretization of the system. Whereas this study makes use of the STS and HTS discrimination suggested and studied by Briggs et al. (2009) due to its tested field methodology, the potential exists for the application of other forms of multiple storage zone systems such as multiple STS or HTS zones in series (Nested), parallel (Competing), or extended combinations thereof. For example, a system could be conceptualized as having a nested two HTS model structure, where a faster, shallower exchange occurs at the bed and a slower exchange occurs further away. These other constructs would require alternative field methodology in order to constrain and inform the model.

2.3. Metrics

Model parameters are used to develop metrics, which system-scale characterizations and comparisons beyond parameter values alone (Runkel, 2002). Extensive knowledge exists on the effect of hydraulic characteristics, stream topography, heterogeneity, and bed form configuration on transient storage, particularly on hyporheic zone geometry, fluxes, and residence times (e.g. Cardenas et al., 2004; Harvey and Bencala, 1993; Hart et al., 1999; Gooseff et al., 2006). Although some principle controls have been identified and attributed to HTS or STS exchange, the vast majority of research has focused on lumping all parameters into single zone transient storage models (Briggs et al., 2009).

In a single storage zone, residence time can be reflective of time spent within the channel (Mulholland et al., 1994), within the storage zones (Thackston and Schnelle, 1970; Hays et al., 1966), or within the entire system (Hays et al., 1966; Nordin and Troutman, 1980). Mean residence times in storage zones are reflective of the volume and exchange rate into and out of storage zones. Exchange with immobile zones can occur via lateral dispersion (Fischer et al., 1979), turbulent exchange (Ghisalberti and Nepf, 2002; Jirka and Uijttewaai, 2004), and Darcian flow in the case of porous media (Harvey and Bencala, 1993). Differences in mixing scales suggest residence times for STS should be less than for HTS. Though pockets of the STS or HTS may have vastly different residence times (Gooseff et al., 2003), it is generally perceived that the mean STS exchange rate is faster than the mean HTS exchange rate (Briggs et al., 2009). Conventional model solutions simulating transient storage are more sensitive to short-time scales and large-mass transfer, indicating that the longer timescales of exchange are ignored (Choi et al., 2000; Harvey et al., 1996; Wagner and Harvey, 1997; Wörman and Wachniew, 2007). As a result, the late-time behavior of tracer test breakthrough curves (BTC) is expected to be influenced most by hyporheic exchange (Gooseff et al., 2003; Haggerty et al., 2000, 2002) models have the potential to describe late-time behavior more accurately than 1-SZ models, because of the ability to separate the STS's fast and the HTS's slow exchange processes. However, as noted by Choi et al. (2000) in-stream tracer BTC data alone is not sufficient to fully inform a 2-SZ solute transport model. To circumvent these limitations Briggs et al. (2009) adopt an approach in which STS size is estimated from direct field measurements and tracer BTCs from STS and from the channel are both fit by the 2-SZ model.

2.3.1. Mean travel time

Mean travel time, t_{mean} (T) is the residence time for a solute molecule travelling a distance x (L) in a stream. It includes the time within the main channel and any storage zones. The mean travel time for single transient storage zones can be calculated to be (Nordin and Troutman, 1980):

$$t_{mean} = \left(\frac{2D}{U^2} + \frac{x}{U} \right) \left(1 + \frac{A_s}{A} \right) \quad (9)$$

where u is the main channel velocity (L/T), calculated by $u = Q/A$. Following the techniques of Hays et al. (1966), the C2-SZ and N2-SZ mean travel times were computed to be:

$$t_{mean,C} = t_{mean,N} = \left(\frac{2D}{U^2} + \frac{x}{U} \right) \left(1 + \frac{A_{STS}}{A} + \frac{A_{HTS}}{A} \right) \quad (10)$$

2.3.2. Storage zone residence time

Another metric that can be useful in comparing and contrasting solute transport models is the mean residence time in the storage zones, T_{sto} (T). It represents the average time that a solute molecule spends in a given storage zone. This residence time can be deter-

mined analytically from the transient storage equations for the storage zones (Hays et al., 1966). The residence time is evaluated using the moments of an impulse response of the concentration in a storage zone. The use of a lower case t for mean travel time and upper case T for residence time is consistent with the work of Runkel (2002) and upheld here for continuity. The average time a solute molecule will stay in a storage zone in the 1-SZ model is given by (Thackston and Schnelle, 1970):

$$T_{sto} = \frac{A_s}{\alpha A} \quad (11)$$

For the competing 2-SZ model, the STS storage residence time is:

$$T_{STS,C} = \frac{A_{STS}}{\alpha_{STS} A} \quad (12)$$

and the HTS storage residence time is:

$$T_{HTS,C} = \frac{A_{HTS}}{\alpha_{HTS} A} \quad (13)$$

Similarly for the nested 2-SZ model, the HTS storage zone residence time is:

$$T_{HTS,N} = \frac{A_{HTS}}{\alpha_{HTS} A_{STS}} \quad (14)$$

and the STS storage zone residence time is:

$$T_{STS,N} = \frac{1}{\alpha_{HTS} + \frac{\alpha_{STS} A}{A_{STS}}} \quad (15)$$

The total nested 2-SZ storage zone residence time, which represents the combined influence of the sequential STS and HTS storage, is given by

$$T_{sto,N} = \left(1 + \frac{A_{HTS}}{A_{STS}} \right) \frac{A_{STS}}{\alpha_{STS} A} \quad (16)$$

There is not an equivalent derivation for the total competing 2-SZ storage zone residence time because in the Competing model structure the two storage zones do not interact. The total storage zone residence time is the amount of time a particle spends in storage before it reenters the stream; therefore, in the case of the Competing model structure, this is not the summation of $T_{STS,C}$ and $T_{HTS,C}$, as the particle will have spent time in the stream between exiting and entering storage zones.

2.3.3. Main channel residence time

Mulholland et al. (1994) provided a metric for the average distance a solute molecule travels within the main channel before entering the storage zone.

$$L_s = \frac{u}{\alpha} \quad (17)$$

Mulholland et al. (1997) defines the residence time of a solute molecule within the main channel of a stream as the inverse of the exchange coefficient. Runkel (2002) derives the main channel residence time by dividing both sides of Equation (17) by u to get

$$T_{str} = \frac{1}{\alpha} \quad (18)$$

For the competing model structure, a solute molecule can leave the main channel and enter either the HTS or STS zone. Similar to equation (17), the average distances a solute molecule travels within the main channel before entering either of the two storage zones can be defined as

$$L_{s,C} = \frac{u}{\alpha_{STS} + \alpha_{HTS}} \quad (19)$$

Dividing both sides of (19) by u we obtain the competing 2-SZ main channel residence time as

$$T_{str,C} = \frac{1}{\alpha_{STS} + \alpha_{HTS}} \quad (20)$$

The main channel residence time for the 2-SZ nested model structure needs only to consider the time it takes to enter the STS, because the HTS does not directly exchange with the main channel, and is given by

$$T_{str,N} = \frac{1}{\alpha_{STS}} \quad (21)$$

3. Application

Runkel (1998) developed a finite difference approximation of the steady-state and dynamic equations for the 1-SZ model equations that can be used to simulate the 1-SZ model structure. The numerical counterpart of Eq. (2) can be substituted into the numerical approximation of Eq. (1) thus reducing the number of equations from 2 to 1 (Runkel and Chapra, 1993, 1994). This decoupling process can also be applied to the C2-SZ and N2-SZ model structures, reducing the number of equations from 3 to 1. This eliminates the need to couple the equations and iteratively solve for a solution.

In the 1-SZ equation there are (9) variables: A , A_S , C , C_S , D , Q , q_L , C_L , and α . The single-transient storage equation is used to solve for C and C_S and the optimal simulation is deemed one that best matches simulated C dynamics (magnitude and timing) to those that were measured in the field. Of the remaining 7 variables, Q , q_L , and C_L are often determined prior to the numerical simulation based on empirical data collected during the tracer experiment and A , A_S , D , and α are optimized in order to fit simulated results to observed data. The 2-SZ equations replace A_S , α , and C_S with A_{STS} , A_{HTS} , α_{STS} , α_{HTS} , C_{STS} , and C_{HTS} . Briggs et al. (2009) describe the methodology to procure field data necessary to solve for the C2-SZ model, where (1) breakthrough curves of C_{STS} collected during the tracer experiment are used in combination with the C breakthrough curves to perform the simulation fitting and (2) the A_{STS} is taken as a ratio of A , based on velocity transect measurements. In summary, the 1-SZ model has one constraint (C) and 4 parameters to optimize (A , A_S , D , and α), whereas the 2-SZ models have 3 constraints (C , C_{STS} , and A/A_{STS}), and 5 parameters to optimize (A , A_{HTS} , α_{STS} , α_{HTS} , and D).

The shuffled complex evolution method (SCE-UA) was used to optimize all parameters simultaneously over the global parameter space efficiently and effectively (Duan et al., 1993). The SCE-UA has been effective at calibrating hydrologic stream flow models (Vrugt et al., 2006), but prior to this study had not been applied to stream solute transport models. The SCE-UA method competitively evolves and shuffles a pre-defined number of complexes, which are groups of points spanning the parameter space, while also incorporating global sampling in order to efficiently and thoroughly converge to an optimal parameter set. The SCE-UA was used with an RMSE objective function to fit the simulated downstream MC and STS BTCs to the observed downstream MC and STS BTCs with equal weighting for each data point in each BTC. For the 1-SZ model structure only the lower-boundary MC BTC was used to perform the fitting.

3.1. Site description

The study site is a 460 m 1st-order Reach of Laurel Run upstream of Whipple Dam, Pennsylvania (see Fig. 2). The drainage area is 4.66 km² of valley–ridge topography, old-growth deciduous trees and mountain laurel. Laurel Run is part of the Susquehanna River Basin's Juniata Sub-Basin and the Chesapeake Bay Watershed. The study reach is free of adjoining perennial streams; however there are ephemeral channels at the upstream and downstream ends as well as midpoint. Aside from a parallel gravel road for access to and from Rothrock State Forest and several hunting cabins, the wa-

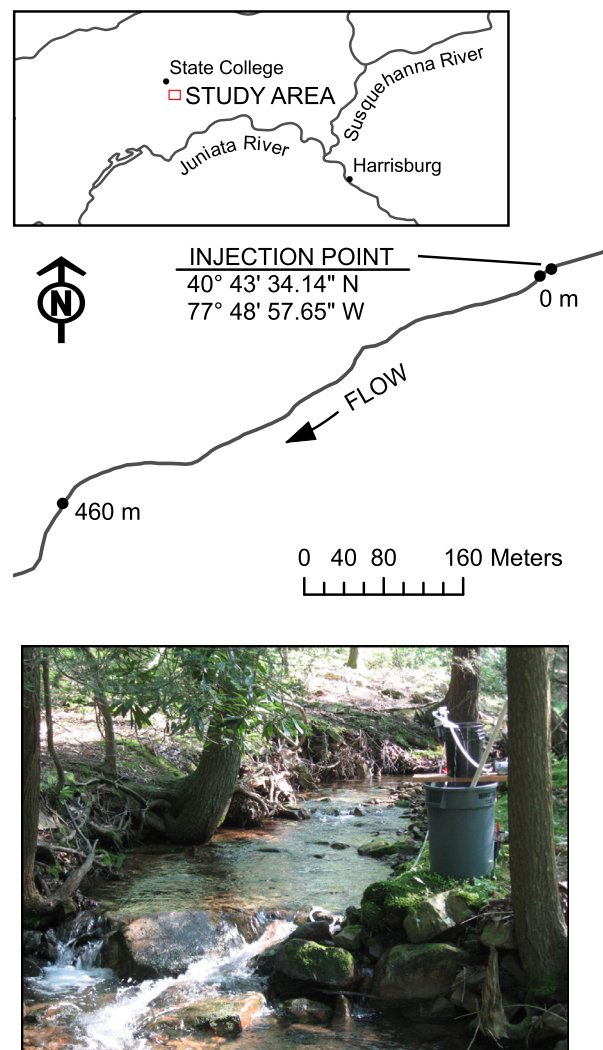


Fig. 2. Experimental Reach of Laurel Run, PA. Injection point (photo) and monitoring locations are indicated.

tershed is free of disturbance. The study site can be characterized as geomorphically diverse with features ranging from steps and pools to riffles, runs, and debris dams. The channel material is mostly cobble, with boulders, gravel, and sand intermixed. The narrow valley and steep basin relief limits the sinuosity of the channel, but the valley floor does occasionally open to allow for intermittent floodplains which in coordination with the debris dams and heavy substrate limits the channel's potential entrenchment.

3.2. Field work

Three tracer experiments, occurring June 25th, July 21st, and August 30th of 2008 were performed using a constant-rate injection of dissolved NaCl as the conservative tracer. Two CR-1000 data loggers each connected to two CS547A conductivity and temperature probes (Campbell Scientific, Inc., Logan, Utah) were placed at 0 m and 460 m along the reach. In accordance with the methods outlined by Briggs et al. (2009), probes from each data logger were placed in the MC and STS zones; conductivity and temperature measurements were collected at 2 s intervals. Conductivity, which was recorded in mS/cm, was corrected for temperature and resistance error along the sensor's cable. The resistance error is a function of the cable length and the cell constant, which are unique to each sensor and cable. The stream's natural baseline conductivity

was determined from the dataset and subtracted. Values were then converted into concentration units of mg/L of Cl^- and lastly the dataset was filtered to reduce its size.

Dilution gauging was used to measure discharge at the upstream and downstream boundary monitoring stations (Payn et al., 2009). The stream was a net gaining stream, thus allowing for a linear lateral inflow to be calculated from the mass balance of each experiment. As a result of this and the removal of the baseline conductivity from each dataset, the inflow concentration was set to zero. Using a Marsh-McBirney model Flomate 2000 wading rod, velocity transect measurements were taken along the reach in order to calculate the ratio of STS area to MC area by identifying the slow moving portions of the section (Briggs et al., 2009). The average A/A_{STS} was 2.0, 2.0, and 2.6 for the June, July, and August Experiments, respectively. The procurement of this ratio and the BTCs in the STS are the only additional field work required for the C2-SZ and N2-SZ models that are not required for the 1-SZ models.

4. Results

4.1. Conceptual study

In order to demonstrate the differences between the N2-SZ and C2-SZ model structures and explore the influence the STS exchange rate has on the BTC in the HTS we studied specific aspects of the model conceptually (Fig. 3). To this end we performed three series of simulations:

- A simulation using the C2-SZ model structure where the parameters were chosen such that the STS BTC fell approximately halfway between the MC and HTS BTCs.
- A simulation using the same parameters as the C2-SZ model in (i), but running the N2-SZ model structure in its place.
- A simulation using the N2-SZ model structure, but where the parameters were optimized to fit the BTCs in the STS and MC to the C2-SZ BTCs in the STS and MC from simulation (i), respectively. In other words, an N2-SZ simulation was optimized to match the C2-SZ simulation.

Clearly, with the same size storage zones and exchange coefficients, the nested model produces lower peak solute concentrations and longer BTC tails in the STS and HTS than for the competing model. Despite the optimization process the MC and STS BTCs for the optimized nested model while similar were not identical to those of the competing model, and that there is a delay in the HTS BTC for the optimized nested model when compare to

the competing model HTS. While α_{HTS} and A_{STS} for the optimized the nested model hardly changed, the α_{STS} increased and the A_{HTS} decreased (Table 1). Consequentially, the STS and HTS mean residence times for the optimized nested model were less than for the competing model, respectively (Table 2). And for the case of identical parameters, the nested model has a lower STS mean residence time and a high HTS mean residence time.

4.2. Numerical simulations of tracer experiments

The fits for the MC were very good for all three model structures, and both the C2-SZ and N2-SZ models fit the STS BTCs well (Fig. 4). Similar to the constant rate-injections performed by Briggs et al. (2009), the BTCs for the STS were very similar to the BTCs for the MC, whereas the BTCs for the HTS were determinably different from the STS and MC BTCs. Fig. 5 illustrates the iterative process of the SCE-UA method for the July 21st experiment using colors to describe the competitive evolution beginning with cold/blue (initial guesses) and ending with hot/red (final optimized value). The model parameter values are summarized in Table 1. The A_{STS} was not optimized as part of the parameter space; rather it was constrained by field measurements of A/A_{STS} , which is the reason for the scalar identicalness of the A and A_{STS} plots.

The results of the SCE-UA method qualitatively highlight parameter space sensitivity. For each of the plots shown in Fig. 5, the rate of convergence to a parameter value over its parameter space indicates the level of confidence in that parameter value. If the scatter has a narrow vertical band then there is high confidence in that parameter but it also means that the error is not very dependent on its value. In contrast, a wide vertical band indicates poor confidence in that parameter value. For example, the A_{STS} for the 2-SZ models both converge earlier to an optimum value than for the 1-SZ model, indicating that there is higher confidence in their parameters. In addition, the convergence for D is relatively poor for both 1-SZ and 2-SZ models, meaning that there is less confidence in D than for the other parameters.

4.3. Residence time metrics

Using the metric formulations presented earlier the residence time metrics for each potential model structure were populated from the three tracer experiment model parameter sets (Table 2). Mean travel residence times, the average time the solute molecule spends in the entire system for a specific length of stream, for the 2-SZ nested model were near identical to the 2-SZ competing model (approximately 0–3% greater), but were between 6% and 23%

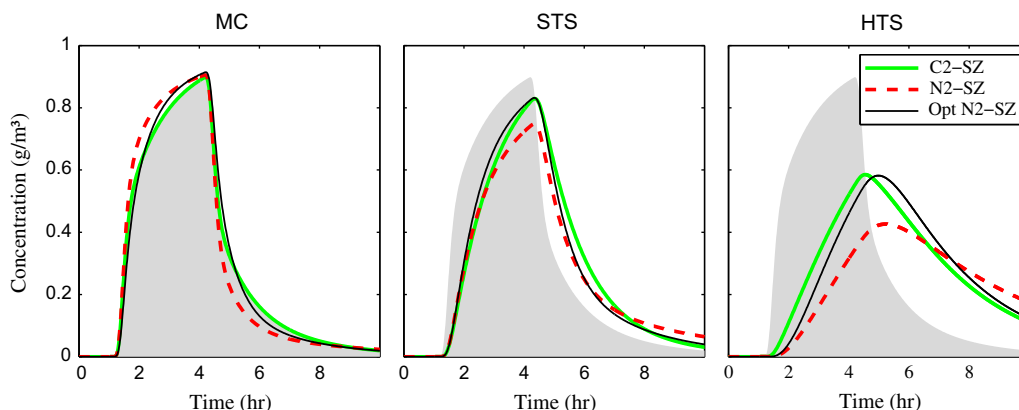


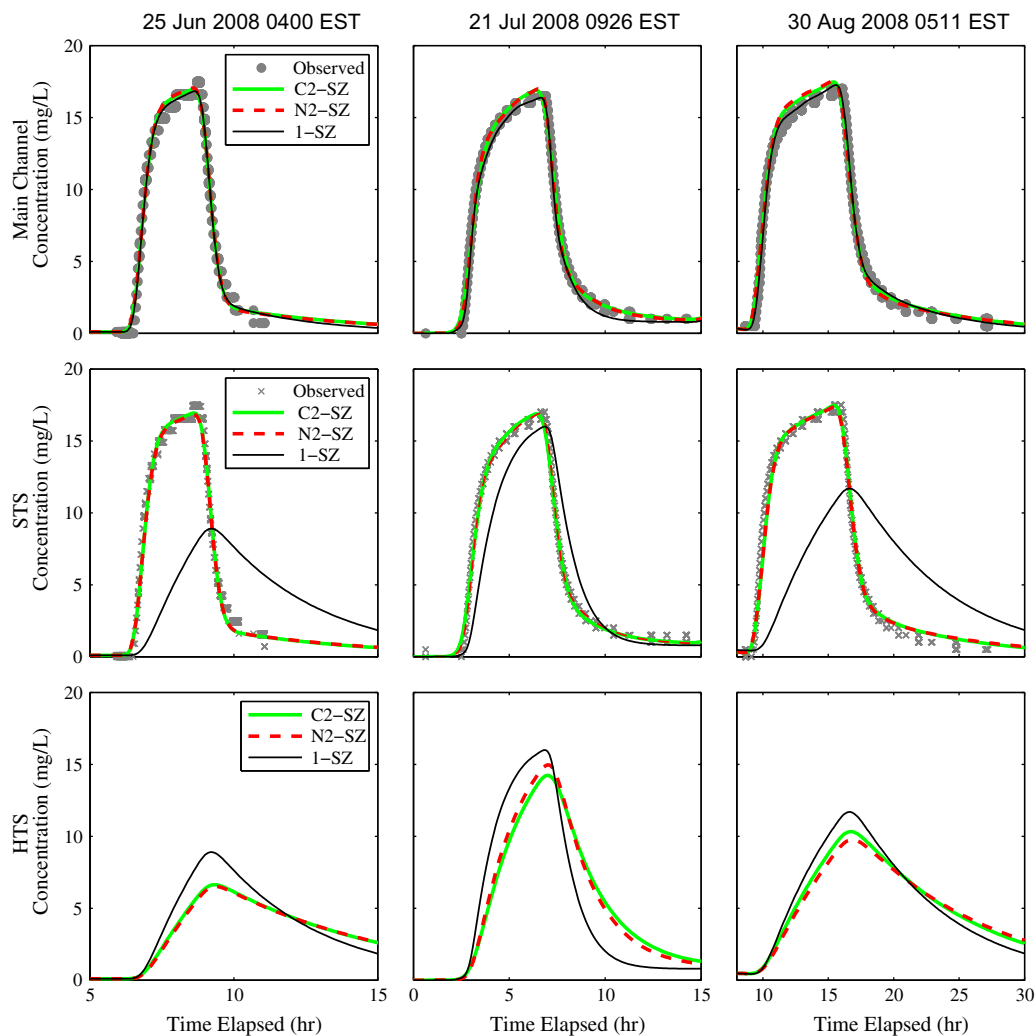
Fig. 3. Conceptual BTC comparison of N2-SZ and C2-SZ models. The MC, STS, and HTS BTCs are shown in the left, middle, and right panels, respectively, with the MC C2-SZ as a gray shadow in all panels (Green – C2-SZ; Dashed red – N2-SZ; Thin black – N2-SZ optimized to fit C2-SZ). (For interpretation of the references to color in this figure legend, the reader is referred to the web version of this article.)

Table 1
Model parameters.

Parameter	6/25/2008			7/21/2008			8/30/2008			Conceptual #1		
	1-SZ	C2-SZ	N2-SZ	1-SZ	C2-SZ	N2-SZ	1-SZ	C2-SZ	N2-SZ	C2-SZ	N2-SZ	N2-SZ optimized
D ($\text{m}^2 \text{s}^{-1}$)	0.831	0.908	1.02	0.201	0.226	0.320	0.503	0.745	0.862	1.0	1.0	1.0
α ($\times 10^{-5} \text{s}^{-1}$)	5.41			11.6			3.73					
α_{STS} ($\times 10^{-5} \text{s}^{-1}$)		438	550		210	240		160	210	30.0	30.0	50.0
α_{HTS} ($\times 10^{-5} \text{s}^{-1}$)		9.19	17.7		8.27	14.9		4.78	11.4	10.00	10.00	10.39
A (m^2)	0.618	0.411	0.418	0.471	0.331	0.339	0.187	0.134	0.137	0.50	0.50	0.55
A_S (m^2)	0.330			0.129			0.125					
A_{STS} (m^2)		0.206	0.209		0.165	0.170		0.0515	0.0529	0.40	0.40	0.44
A_{HTS} (m^2)		0.589	0.606		0.145	0.129		0.151	0.155	0.40	0.40	0.30
RMSE	0.306	0.351	0.353	0.449	0.351	0.354	0.276	0.44	0.464			0.190
u ($\times 10^{-2} \text{m s}^{-1}$)	9.3	14.0	13.8	6.2	8.8	8.6	4.7	6.5	6.4	10.0	10.0	9.1
Q ($\times 10^{-2} \text{m}^3 \text{s}^{-1}$)	5.76			2.90			0.87			5.00		
q_L ($\times 10^{-6} \text{m}^2 \text{s}^{-1}$)	6.38			18.00			0.73			0.00		

Table 2
Residence time metrics.

Metric	6/25/2008			7/21/2008			8/30/2008			Conceptual #1		
	1-SZ	C2-SZ	N2-SZ	1-SZ	C2-SZ	N2-SZ	1-SZ	C2-SZ	N2-SZ	C2-SZ	N2-SZ	N2-SZ optimized
T_{mean} ($\times 10^2 \text{s}$)	7.6	95	98	83	89	89	168	181	187	124	124	123
T_{str} ($\times 10^2 \text{s}$)	185	2.2	1.8	86	4.6	4.2	268	6.1	4.8	25	33	20
T_{sto} ($\times 10^2 \text{s}$)	99		3.6	24		3.7	179		7.2		53	27
T_{STS} ($\times 10^2 \text{s}$)		1.1	0.89		2.4	2.0		2.4	1.8	27	21	14
T_{HTS} ($\times 10^2 \text{s}$)		156	164		53	51		236	257	80	100	66

**Fig. 4.** BTC comparisons of 1-SZ, N2-SZ, and C2-SZ model structures at laurel run for three tracer injection experiments.

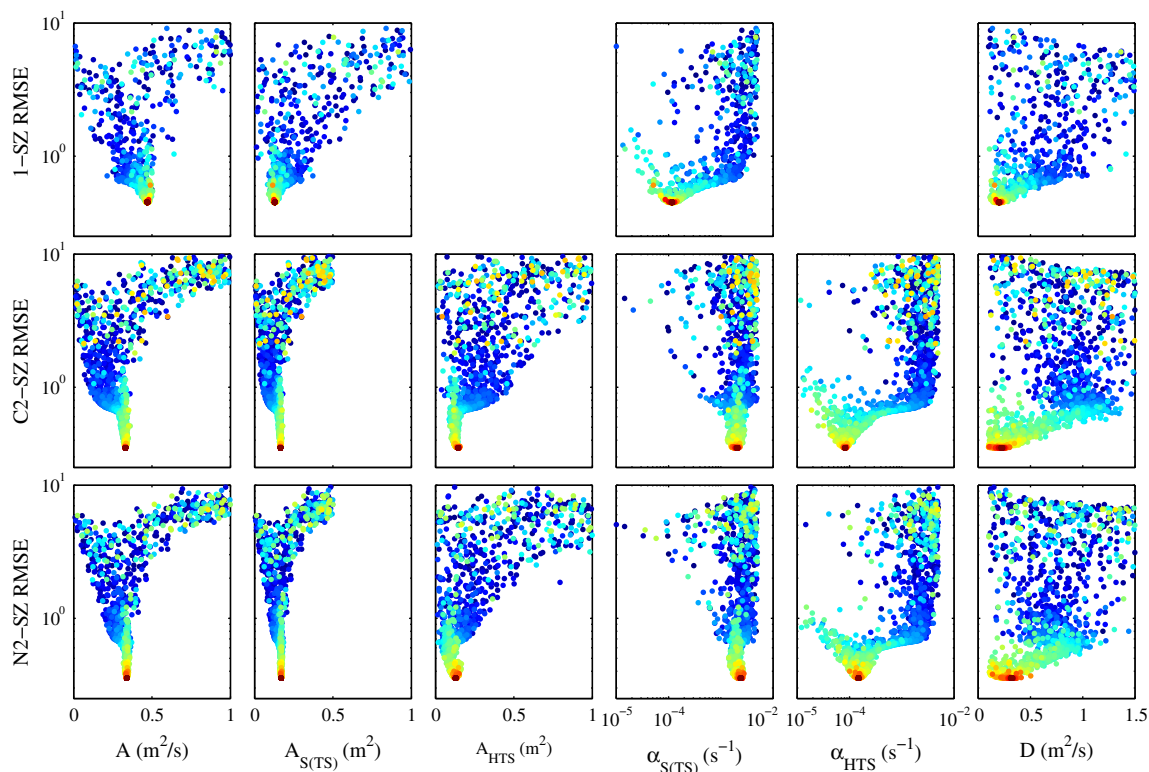


Fig. 5. Color coded parameter optimization for 7/21/2008 experiment (first iteration – blue, last iteration – red). (For interpretation of the references to color in this figure legend, the reader is referred to the web version of this article.)

greater than the 1-SZ model. While expectations might be that t_{mean} should be the same for all models on account of the fact that the same main channel BTC is being fitted, the dissimilarity between the 1-SZ and 2-SZ models can be attributed to the additional STS BTC that the 2-SZ models fit, but that the 1-SZ model does not fit. With regard to mean channel residence time, which is the average time a solute molecule spends within the main channel before entering a storage zone, the $T_{str,N}$ were less than $T_{str,C}$ (9–22%) and significantly less than T_{str} (95–99%).

In the 2-SZ models, storage residence times are computed for each zone, individually, or in the case of the nested model, the combination of both STS and HTS. Beginning with the STS zone, we find that T_{STS} in the nested model is 14–25% less than T_{STS} in the competing model. This is consistent for all three experiments, whereas the residence times in the HTS for the nested model when compared to the competing model were 4% and 5% greater for the June and August experiments, respectively, but 9% less for the July experiment. The residence times in the HTS for both 2-SZ model structures and all three experiments were 22 to 184 times greater than the residence times in the STS. In the case of the nested model structure, a cumulative storage zone residence time can be found that considers the time spent in both the STS and HTS before reentering the main channel. The $T_{sto,N}$ was 1.8 to 4 times greater than T_{STS} , 14–46 times less than $T_{HTS,N}$, and 6–28 times less than T_{sto} . In comparing the storage residence times for the 1-SZ model to each of the 2-SZ models' individual zones, the 1-SZ storage residence times were 10–100 times greater than in the STS but roughly 50–75% less than in the HTS.

5. Discussion

5.1. Feasibility

The field work for both 2-SZ models is identical, requiring little more effort than the 1-SZ model, and the fitting of modeled data to observed data for all three models showed similar confidence in

parameter optimization, advocating that differences in methodology should not be a determining factor in model selection. The requirement that the models accurately reproduce the BTC in the main channel was met by all three models; however, if the objective of the modeling exercise was to discriminate between the main channel and STS, then the 1-SZ model is likely not appropriate. For all three experiments, the modeled BTC of the storage zone for the 1-SZ model did not match the observed BTC in the STS, whereas for the 2-SZ models, the modeled BTCs in the MC and STS matched the observed BTCs in the MC and STS, respectively. The 1-SZ model is best-suited to characterize streams with a gross propensity to one type of storage, either STS or HTS, but not both; similar findings were presented by Choi et al. (2000). In these experiments, the observed BTCs in the STS showed very little lag time behind the observed BTCs in the MC, falsely suggesting that the STS BTC could be lumped with the MC BTC and that the 1-SZ model's storage zone BTC represents the HTS BTC. There are two possible shortcomings with the MC and STS lumping: (1) the STS and MC may be subject to different biogeochemical processing which the 1-SZ cannot discriminate, and (2) there exists a lag between the MC and STS BTCs which is not well illustrated in Fig. 4 due to the scale of a constant-rate injection, but similarly can be seen more clearly in the slug injections shown by Briggs et al. (2009). The delay in the STS BTC is unmistakably less than the delay for the HTS BTC, indicating that exchange is much faster in the STS and that there is a direct connection of exchange between the STS and MC. The presence and contribution of the HTS must be determined from the numerical model; whereas the presence of the STS can be identified through field measurements such as the ratio of non-advective area to advective area and experimental BTCs.

Application of the 1-SZ model requires the fitting of one BTC, that observed in the MC, whereas the 2-SZ models requires fitting of two BTCs, that observed in the MC and STS. In the three experiments in this study, the observed STS BTC was very close to the observed MC BTC, but there was still an observable delay. Due to

the fast exchange between the MC and STS, the differences in model structure were not accentuated resulting in modeled BTCs in the HTS that were very similar for both the C2-SZ and N2-SZ models. Analytically, it can be shown that both 2-SZ models can create identical BTCs for the MC, STS, and HTS if the STS is either identical to the MC or to the HTS, but not if the STS BTC is dissimilar to both.

Fig. 3 demonstrates that when a BTC for an STS does not match the MC or HTS breakthrough curves, the C2-SZ and N2-SZ models with identical parameters do not result in matching BTCs for the MC, STS, or HTS. One striking difference between the C2-SZ and N2-SZ models with identical parameters is the difference in shape of the STS and HTS BTCs. The STS and HTS BTCs of the N2-SZ model with identical parameters has lower peak and a longer tail than the C2-SZ models STS and HTS BTCs, respectively, owing to the compounding delay caused by its model structure. Another key aspect of this figure is the inability of the N2-SZ model with optimized parameters to perfectly recreate the BTCs of the C2-SZ model. The differences in model structure are accentuated when the STS BTC diverges from the MC or HTS BTC. The optimized BTCs of the N2-SZ, despite matching the peaks of the C2-SZ BTCs, feature a noticeable delay in the HTS and a faster exchange in the HTS.

The ability to accurately simulate observed BTCs in the main channel and STS, when they are this similar, does not confirm the fidelity of either 2-SZ model, rather it only confirms the potential for each model to mimic the total system output. The C2-SZ and N2-SZ represent two extremes of a 2-SZ model structure. A third model in which each zone would interact with each other and the main channel would perhaps be more representative of the physical nature of a stream system. However, this third model would have to include both $\alpha_{HTS,C}$ and $\alpha_{HTS,N}$, thereby increasing the number of parameters to optimize and thus negating the method developed by Briggs et al. (2009) that can be used to populate these parameters and heighten the risk of over-fitting data due to availability of more free parameters rather than actually matching physical processes.

5.2. Interpretation of parameters

The optimization process we used provides insight into the sensitivity of the model parameters to the model structure. The SCE-UA method showed strength in optimizing each parameter for all three model structures, as evident by the close fitting of the BTCs and the convergence of the values. The narrow fitting of the area parameters for the 2-SZ models in comparison to the 1-SZ model highlights greater confidence and sensitivity. The 1-SZ had a greater main channel area, less total storage area, and less total system area than the 2-SZ models, which both had similar values of A , A_{STS} , and A_{HTS} . The difference in areas between the 1-SZ and 2-SZ models has potential implications about the physical validity and interpretation of the model as the simulation's velocity in the main channel, u , is defined by the advective term as Q/A , of which discharge is constant between all models. Therefore, the addition of a second storage zone increases the estimated mean velocity in the main channel. This is a measureable physical difference that could be used to improve model selection, but was not examined in this study.

Even though the 1-SZ model lumps all storage into a single zone, this present study demonstrated that the 2-SZ model does not simply parse the 1-SZ model's storage area, A_S into A_{STS} and A_{HTS} ; rather it also parses area from the main channel and that total system area was not identical between the 1-SZ and 2-SZ models. In both 2-SZ models, the STS has less lag and faster exchange than the HTS, so the reduction in A in the 2-SZ model can be attributed primarily to the addition of the STS. Both 2-SZ models resulted in slightly higher values for D , α_{STS} , and α_{HTS} , with slightly faster exchange occurring in the N2-SZ model. To offset the higher exchange rates, the total storage area increased for the 2-SZ models, with the 2-SZ A_{HTS} consistently eclipsing the 1-SZ A_S . These differences highlight that model

parameters are sensitive to model structure, and whereas differences in 2-SZ models may appear to be small, the most striking difference is the consistently faster exchange rates for the N2-SZ.

5.3. Interpretation of residence time and flow path differences

Each model structure poses a unique set of conditions that should be interpreted alongside residence times, which is a physical characteristic that can directly influence biogeochemical processing. The mean travel time, the time spent in the whole system, was determined to be the same for both 2-SZ models. This is in agreement with the analytical derivations, the metric populated with the optimized parameters, and the breakthrough curve. We had expected that the mean travel time computed for the 1-SZ model would also match the 2-SZ models; however it did not and rather, it was consistently less. This may be attributed to the 1-SZ model being constrained to one observed BTC, whereas the 2-SZ models were constrained to two observed BTCs. In order for the 1-SZ model to have a lower mean travel time than the 2-SZ models, because as mentioned previously it had a lower mean velocity, it would need to counter with either a higher T_{str} or a lower T_{sto} , which it did in both cases. The T_{str} showed a substantial difference between the 1-SZ and 2-SZ models as well between the N2-SZ and C2-SZ models. The 1-SZ model conceptualizes that a solute molecule travels downstream continuously without stopping in an immobile zone for much longer than in the 2-SZ models, because in the 2-SZ models, the fast exchange between the STS and MC would force solute molecules to rest more frequently. In the N2-SZ model, all stored solute molecules must pass through the STS zone, so the N2-SZ model has a larger α_{STS} than the C2-SZ model, in which stored solute molecules can connect directly from the stream to their storage zone.

Residence time in the STS is also influenced by model structure. Solute molecules transported in a C2-SZ model are not required to pass through the STS prior to entering the HTS as the zones are independent of each other. Solute molecules can spend time in both zones, but are highly unlikely to re-enter a zone at the same stream location (as soon as a solute molecule leaves the storage zone it is transported downstream), therefore the residence times are not cumulative. The average residence time for the nested storage system, $T_{sto,N}$ which accounts for the average time spent in the STS/HTS combination before reentering the main channel is considerably less than the time for the 1-SZ model, T_{sto} and somewhere between the N2-SZ T_{STS} and T_{HTS} . In the nested model structure, solute molecules entering the HTS will have spent time within the STS already and will have to do so again when leaving the HTS. Not all solute molecules entering the STS must pass through the HTS as solute molecules can re-enter the main channel without entering the HTS. This is also true of solute molecules exiting the HTS, as solute molecules can exit the HTS and re-enter the HTS at the same stream location without entering the main channel. There are more options for solute molecule paths in the nested 2-SZ model structure and therefore individual solute molecule residence times can be compounded with each cycle. Considering the circular nature of the N2-SZ model, a solute molecule could have multiple entries into the STS without reentering the main channel thus eclipsing the residence time for the C2-SZ model, despite the finding that the average STS residence time was found to be greater in the C2-SZ model than in the N2-SZ model. The potential for zonal cycling in the N2-SZ model is a significant feature not described by either the residence time metrics or the BTCs.

5.4. Consideration of mass

While the BTCs, parameters, residence time, and path highlight differences in the models, the significance of the model structure's

influence can be assessed by the percentage of mass in the system that is stored vs. the portion transported. For each model structure, the net mass flow rates at the 460 m station for the STS, HTS, and MC are illustrated in Fig. 6 along with the main channel's advective, dispersive, and storage components. There is a striking similarity between the 1-SZ, N2-SZ and C2-SZ models for the MC and the main channel's advective and dispersive components, but only the C2-SZ and N2-SZ continue that similarity for the STS, HTS, and main channel's storage component. These results demonstrate that the 1-SZ model affects the mass flow rate storage differently than the 2-SZ models, in which both the C2-SZ and N2-SZ are similar.

For each model structure, an approximation of mass entering each of the system zones (MC, STS, and HTS) was made by integrating the positive sign values of the net mass flow rate over time. The ratio of mass entering storage vs. the main channel was plotted against the residence time of that storage zone (Fig. 7). For each experiment, the N2-SZ and C2-SZ points for the STS are clumped together with a lower residence time than the N2-SZ and C2-SZ points for the HTS which are also clumped together. The 1-SZ curves consistently have a lower mass ratio than either of the 2-SZ's HTS and STS curves, but always a higher residence time than the STS points, demonstrating that there is less mass being stored in the 1-SZ model than in the 2-SZ models, which has major biogeochemical processing implications. Furthermore, aside from path, higher N2-SZ STS exchange, and zonal cycling potential, this study was not able to identify major quantifiable differences to discern appropriateness between the two 2-SZ model structures, which suggests that aside from the expectation that more research is necessary; the interpretation of the system's conceptual connections should be the primary driver in structure selection.

5.5. Reactive tracer simulations

To assess the potential influence model structure has on biogeochemical processes, simulations were performed of hypothetical first-order reaction rate combinations of 0.001 s⁻¹ and 0.01 s⁻¹ in each of the storage zones: λ_{STS}, for the STS and λ_{HTS}, for the HTS. These values fall within a reasonable range of reaction rate time-scales for biogeochemical processes between denitrification and oxygen consumption (Gooseff et al., 2003). Using the calibrated parameters for the August experiment, the following three hypothetical scenarios were run and compared to the non-reactive case (Fig. 8):

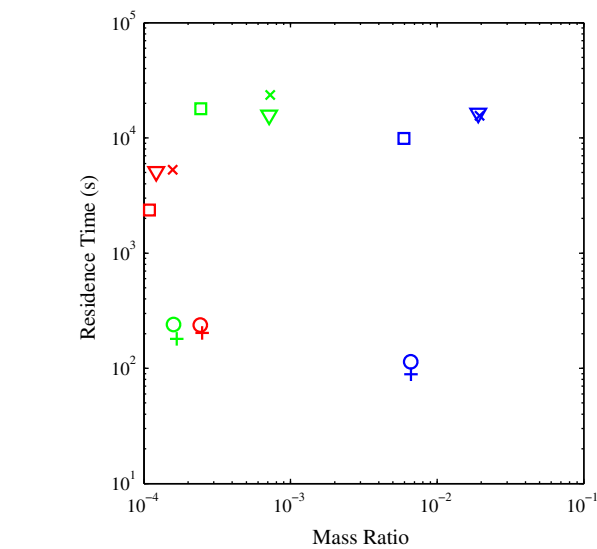


Fig. 7. Comparison of residence time to net mass entering storage zone relative to main channel (Colors: Blue – 6/25/2008; Red – 7/21/2008; Green – 8/30/2008) (Shapes: ○ – C2-SZ STS; × – C2-SZ HTS; + – N2-SZ STS; ▽ – N2-SZ HTS; □ – 1-SZ). (For interpretation of the references to color in this figure legend, the reader is referred to the web version of this article.)

$\lambda_{STS} = \lambda_{HTS}$	$\lambda = 0$	$\lambda_{STS} = 0.001$	$\lambda_{HTS} = 0.001$
$\lambda_{STS} < \lambda_{HTS}$	$\lambda = 0$	$\lambda_{STS} = 0.001$	$\lambda_{HTS} = 0.01$
$\lambda_{STS} > \lambda_{HTS}$	$\lambda = 0$	$\lambda_{STS} = 0.01$	$\lambda_{HTS} = 0.001$

The scenarios modeled examine cases where it is hypothetically expected for biogeochemical reactions to differ depending on which zone the tracer is located. In all cases presented, a zero reaction rate was applied to the main channel, so as to not distract from the influences of the storage zones and the differences in model structure.

Physically, a greater reaction coefficient translates to a faster reactive decay of a tracer, so in case 2 the tracer decays faster in the HTS than in the STS, whereas in case 3 the tracer decays faster in the STS than in the HTS. From the results, the non-conservative case shows nearly identical BTCs of the main channel and STS and a

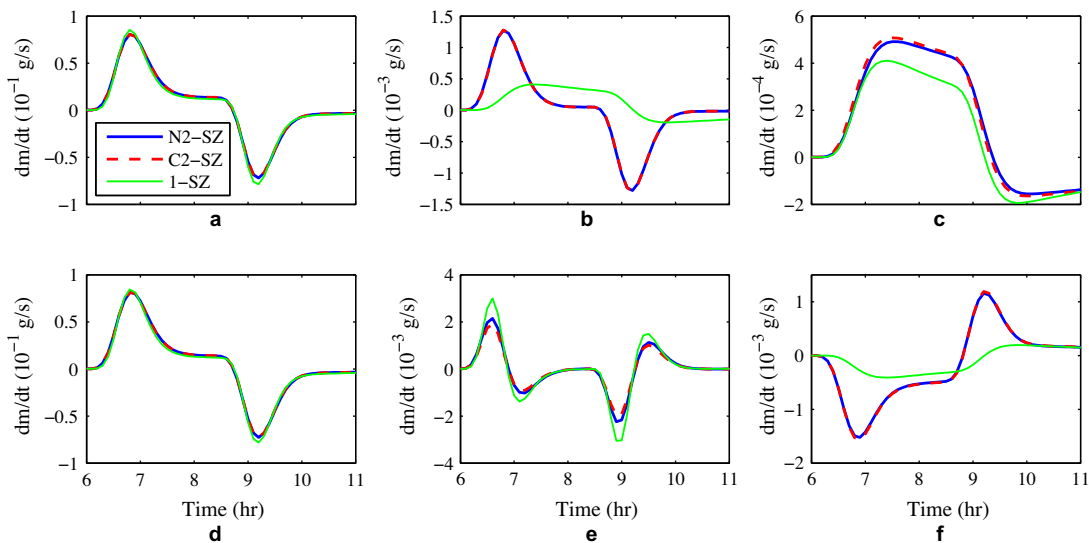


Fig. 6. Net mass flow rate for June at laurel run station 460 m, beginning at 6/25/2008 4:00 AM EST (Panels: a – main channel; b – STS; c – HTS; d – advection; e – dispersion; f – storage) flux for the 1-SZ model's storage zone is shown in both panels B and C.

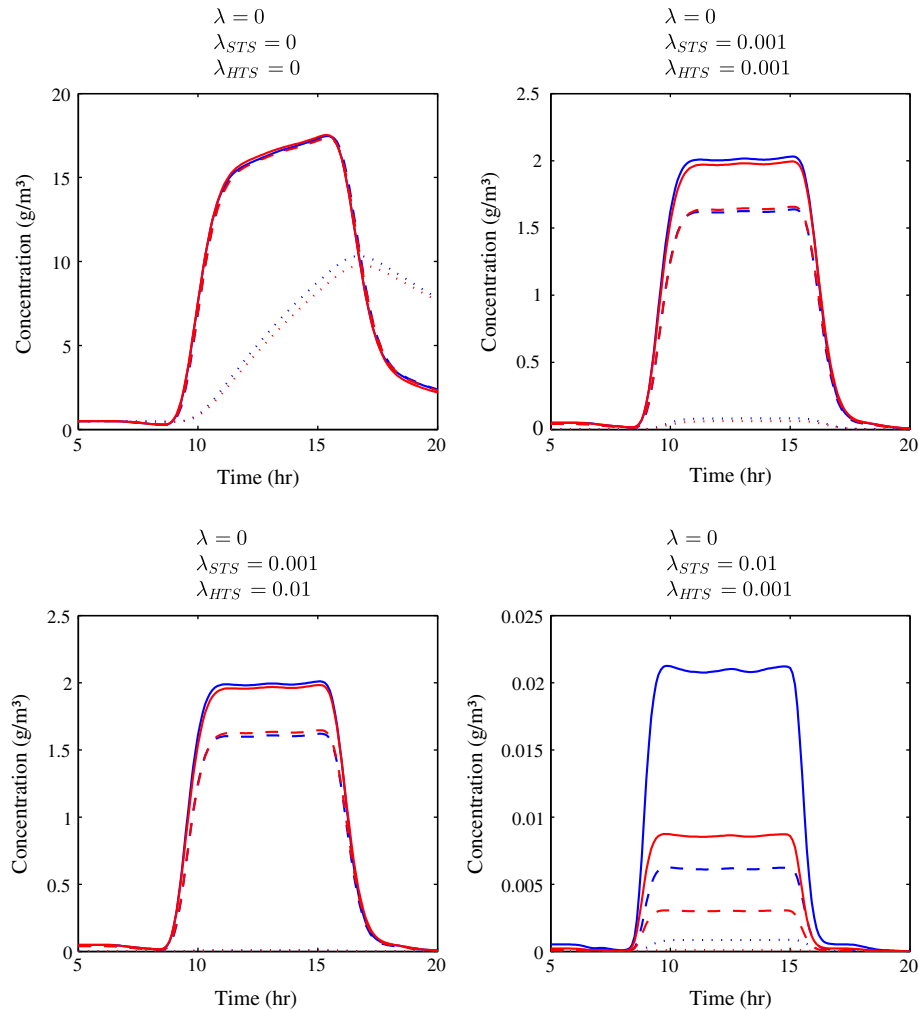


Fig. 8. Conceptual comparison of main channel (solid), STS (dashed), and HTS (dotted) BTCs for reactive tracers with varying decaying coefficients for both N2-SZ (red), and C2-SZ (blue) model structures. (For interpretation of the references to color in this figure legend, the reader is referred to the web version of this article.)

lagged HTS for both model structures. In the case with identical reaction rates for the STS and HTS, a distinct difference is now seen between the main channel and STS in addition to a general decrease in overall concentration, a flattening of the BTCs, and marked reduction in the lag and skew of the HTS BTC. From these BTCs, it can be seen that the reaction coefficients are high enough to prevent re-contribution of the tracer to the main channel from the storage zones.

In the case where λ_{STS} is less than λ_{HTS} the BTCs for the main channel and STS are very similar for both model structures and nearly identical to the BTCs presented in the case with identical reaction rates, but the HTS BTCs are significantly reduced. The higher reaction rates for the HTS did not influence the BTCs for the main channel or STS for either model structure. This is in stark contrast for the last case, where the λ_{STS} is greater than the λ_{HTS} . Here the BTCs for the main channel, STS, and HTS are different between the model structures; the C2-SZ model structure has higher concentration levels for each zone than the N2-SZ model. In the N2-SZ model the STS exchange rate is greater than for the C2-SZ model, because all mass passes through the STS, which when combined with λ_{STS} greater than λ_{HTS} results in a greater potential for mass decay than in the C2-SZ model. While simulations of conservative tracers did not produce dramatically different BTCs for the experimental cases, these simulations of reactive tracers show that choice of model structure can have significant consequences when dealing with reactive tracers even when conservative tracers do

not. If a reactive tracer was to be used to determine zone-specific reaction rates, then the calibrated values would be dependent on the model structure selected.

6. Conclusions

We investigated the influence of model structure in one-dimensional stream solute transport models with transient storage for a 1st order stream in central Pennsylvania. Three conceptual model structures were studied: a single transient storage zone (1-SZ) model, a Competing two transient storage zone (C2-SZ) model where each storage zone interacts with the stream but not with each other, and a nested two storage zone (N2-SZ) model where the one of the storage zones acts as an intermediary between the stream and the other storage zone. Multiple storage zone models were developed to represent in-channel surface transient storage (STS) and hyporheic transient storage (HTS) separately to overcome the limitations of single storage zone (1-SZ) models. The results of this study suggest that even though all three models can be used to fit in-stream tracer experiment data, models should be selected based on the interpretation of the system. Both 2-SZ model structures have the ability to discriminate transport processes between different zones, but for our field site experiments it was not determinable from the tracer experiments if one model was more appropriate. For each of these three models, solute would travel uniquely

different paths, as the structure determines the process by which solute molecules pass through zones and for how long they would remain in them. This is not well-illustrated by the BTCs alone for a conservative tracer, especially in the case of N2-SZ model's zonal cycling capability, but can be better illustrated through the use of reactive tracers. Model structure also affected optimized parameter values for area and exchange, and has the potential to change the shape and lag of the HTS BTC. A study of a hypothetical reactive tracer also showed that calibration of zone specific reaction rate coefficients will be dependent on model structure selection; and that reactions in the STS, more so than the HTS, compound the influence model structure has on system impacts. We found that the differences in conceptual transient storage interactions are significant to the interpretation of residence times, because metrics and BTCs alone do not well describe the potential for zonal cycling in the N2-SZ. Thus our interpretation of zonal interaction may play an important role in discrimination of biogeochemical processes within each zone and recommend that work continue to address the appropriateness of model structure selection.

Acknowledgements

This study was funded by the Pennsylvania Water Resources Research Institute. The authors are grateful to the land managers of Rothrock State Park for supporting our work, and to 3 anonymous reviewers.

References

- Anderson, J.K., Wondzell, S.M., Gooseff, M.N., Haggerty, R., 2005. Patterns in stream longitudinal profiles and implications for hyporheic exchange flow at the H.J. Andrews Experimental Forest, Oregon, USA. *Hydrol. Process.* 19 (15), 2931–2949.
- Bencala, K.E., Walters, R.A., 1983. Simulation of solute transport in a mountain pool-and-riffle stream: a transient storage model. *Water Resour. Res.* 19 (3), 718–724.
- Bottacin-Busolin, A., Marion, A., Musner, T., Tregnaghi, M., Zaramella, M., 2011. Evidence of distinct contaminant transport patterns in rivers using tracer tests and a multiple domain retention model. *Adv. Water Res.* 34, 737–746. <http://dx.doi.org/10.1016/j.advwatres.2011.03.005>.
- Briggs, M.A., Gooseff, M.N., Arp, C.D., Baker, M.A., 2009. A method for estimating surface transient storage parameters for streams with concurrent hyporheic storage. *Water Resour. Res.* 45, W00D27, doi:<http://dx.doi.org/10.1029/2008WR006959>.
- Briggs, M.A., Gooseff, M.N., Peterson, B.J., Morkeski, K., Wollheim, W.M., Hopkinson, C.S., 2010. Surface and hyporheic transient storage dynamics throughout a coastal stream network. *Water Resour. Res.* 46, W06516. <http://dx.doi.org/10.1029/2009WR008222>.
- Cardenas, M.B., Wilson, J.L., Zlotnik, V.A., 2004. Impact of heterogeneity, bed forms, and stream curvature on subchannel hyporheic exchange. *Water Resour. Res.* 40, W08307. <http://dx.doi.org/10.1029/2004WR003008>.
- Donado, L.D., Sanchez-Vila, X., Dentz, M., Carrera, J., Bolster, D., 2009. Multicomponent reactive transport in multicontinuum media. *Water Resour. Res.* 45, W11402. <http://dx.doi.org/10.1029/2008WR006823>.
- Duan, Q.G., Gupta, V.K., Sorooshian, S.J., 1993. A shuffled complex evolution approach for effective global optimization. *J. Optim. Theory Appl.* 76, 501–521.
- Choi, J., Harvey, J.W., Conklin, M.H., 2000. Characterizing multiple timescales of stream and storage zone interaction that affect solute fate and transport in streams. *Water Resour. Res.* 36 (6), 1511–1518.
- Fischer, H., List, E., Koh, R., Imberger, J., 1979. *Mixing in Inland and Coastal Waters*, New York.
- Ghisalberti, M., Nepf, H.M., 2002. Mixing layers and coherent structures in vegetated aquatic flows. *J. Geophys. Res.* 107 (C2 3011), 1–11.
- Gooseff, M.N., Wondzell, S.M., Haggerty, R., Anderson, J., 2003. Comparing transient storage modeling and residence time distribution analysis in geomorphically varied reaches in the Lookout Creek basin, Oregon USA. *Adv. Water Resour.* 26 (9), 925–937.
- Gooseff, M.N., McKnight, D.M., Runkel, R.L., Duff, J.H., 2004. Denitrification and hydrologic transient storage in a glacial meltwater stream, McMurdo Dry Valleys, Antarctica. *Lim. Oceanogr.* 49 (5), 1884–1895.
- Gooseff, M.N., LaNier, J., Haggerty, R., Kokkeler, K., 2005. Determining in-channel (dead zone) transient storage by comparing solute transport in a bedrock channel–alluvial channel sequence Oregon. *Water Resour. Res.* 41 (6), W06014.
- Gooseff, M.N., Anderson, J.K., Wondzell, S.M., LaNier, J., Haggerty, R., 2006. A modeling study of hyporheic exchange pattern and the sequence, size, and spacing of stream bedforms in mountain stream networks, Oregon USA. *Hydrol. Process.* 20 (11), 2443–2457.
- Haggerty, R., Gorelick, S.M., 1995. Multiple-rate mass transfer for modeling diffusion and surface reactions in media with pore-scale heterogeneity. *Water Resour. Res.* 31 (10), 2383–2400. <http://dx.doi.org/10.1029/95WR10583>.
- Haggerty, R., McKenna, S.A., Meigs, L.C., 2000. On the late-time behavior of tracer test breakthrough curves. *Water Resour. Res.* 36 (12), 3467–3479.
- Haggerty, R., Wondzell, S.M., Johnson, M.A., 2002. Power-law residence time distribution in the hyporheic zone of a 2nd-order mountain stream. *Geophys. Res. Lett.* 29 (13), 18–18-4.
- Hart, D.R., Mulholland, P.J., Marzolf, E.R., DeAngelis, D.L., Hendricks, S.P., 1999. Relationships between hydraulic parameters in a small stream under varying flow and seasonal conditions. *Hydrol. Process.* 13, 1497–1510.
- Harvey, J.W., Bencala, K.E., 1993. The effect of streambed topography on surface–subsurface water exchange in mountain catchments. *Water Resour. Res.* 29 (1), 89–98.
- Harvey, J.W., Wagner, B.J., Bencala, K.E., 1996. Evaluating the reliability of the stream tracer approach to characterize stream–subsurface water exchange. *Water Resour. Res.* 32 (8), 2441–2451.
- Harvey, J.W., Saiers, J.E., Newlin, J.T., 2005. Solute transport and storage mechanisms in wetlands of the Everglades, south Florida. *Water Resour. Res.* W05009. <http://dx.doi.org/10.1029/2004WR003507>.
- Hays, J.R., Krenkel, P.A., Schnelle, K.B., 1966. Mass transport mechanisms in open-channel flow, Vanderbilt Univer., Nashville, Tenn.
- Jirka, G.H., Uijttewaal, W.S.J., 2004. Shallow Flows: a Definition", in "Shallow Flows", A.A. Balkema, Roderdam, The Netherlands.
- Marion, A., Zaramella, M., Bottacin-Busolin, A., 2008. Solute transport in rivers with multiple storage zones: the STIR model. *Water Resour. Res.* 44, W10406. <http://dx.doi.org/10.1029/2008WR007037>.
- Mulholland, P.J., Marzolf, E.R., Webster, J.R., Hart, D.R., Hendricks, S.P., 1997. Evidence that hyporheic zones increase heterotrophic metabolism and phosphorus uptake in forest streams. *Limnol. Oceanogr.* 42 (3), 443–451.
- Mulholland, P.J., Steinman, A.D., Marzolf, E.R., Hart, D.R., DeAngelis, D.L., 1994. Effect of periphyton biomass on hydraulic characteristics and nutrient cycling in streams. *Oecologia* 98 (1), 40–47.
- Nordin Jr., C.F., Troutman, B.M., 1980. Longitudinal dispersion in rivers; the persistence of skewness in observed data. *Water Resour. Res.* 16 (1), 123–128.
- Payn, R.A., Gooseff, M.N., McGlynn, B.L., Bencala, K.E., Wondzell, S.M., 2009. Channel water balance and exchange with subsurface flow along a mountain headwater stream in Montana, United States. *Water Resour. Res.* 45, W11427. <http://dx.doi.org/10.1029/2008WR007644>.
- Runkel, R.L., Chapra, S.C., 1993. An efficient numerical solution of the transient storage equations for solute transport in small streams. *Water Resour. Res.* 29 (1), 211–215.
- Runkel, R.L., Chapra, S.C., 1994. Reply to comment on 'An efficient numerical solution of the transient storage equations for solute transport in small streams' by W.R. Dawes and David Short. *Water Resour. Res.* 30 (10), 2863–2865.
- Runkel, R.L., 1998. One-dimensional transport with inflow and storage (OTIS): a solute transport model for streams and rivers. US Geological Survey Water-Resources Investigation Report 98-4018, Denver, CO.
- Runkel, R.L., 2002. A new metric for determining the importance of transient storage. *J. North. Am. Benthol. Soc.* 21, 529–543. <http://dx.doi.org/10.2307/1468428>.
- Runkel, R.L., McKnight, D.M., Rajaram, H., 2003. Modeling hyporheic zone processes. *Adv. Water Resour.* 26, 901–905.
- Stewart, R.J., Wollheim, W.M., Gooseff, M.N., Briggs, M.A., Jacobs, J.M., Peterson, B.J., Hopkinson, C.S., 2011. Separation of river network-scale nitrogen removal among the main channel and two transient storage compartments. *Water Resour. Res.* 47, W00J10, doi:<http://dx.doi.org/10.1029/2010WR009896>.
- Thackston, E.L., Krenkel, P.A., 1967. Longitudinal mixing in natural streams. *J. Sanit. Eng. Div. Am. Soc. Civ. Eng.* 93 (SA5), 67–90.
- Thackston, E.L., Schnelle Jr., K.B., 1970. Predicting effects of dead zones on stream mixing. *J. Sanit. Eng. Div. Am. Soc. Civ. Eng.* 96 (SA2), 319–331.
- Vannote, R.L., Minshall, G.W., Cummins, K.W., Sedell, J.R., Cushing, C.E., 1980. The river continuum concept. *Can. J. Fish. Aquat. Sci.* 37, 130–137.
- Vrugt, J.A., Gupta, H.V., Dekker, S.C., Sorooshian, S., Wagener, T., Bouten, W., 2006. Confronting parameter uncertainty in hydrologic modeling: application of the SCEM-UA algorithm to the Sacramento Soil Moisture Accounting model. *J. Hydrol.* 325, 288–307.
- Wagner, B.J., Harvey, J.W., 1997. Experimental design for estimating parameters of rate-limited mass transfer: analysis of stream tracer studies. *Water Resour. Res.* 33 (7), 1731–1742.
- Willmann, M., Carrera, J., Sanchez-Vila, X., Silva, O., Dentz, M., 2010. Coupling of mass transfer and reactive transport for nonlinear reactions in heterogeneous media. *Water Resour. Res.* 46, W07512. <http://dx.doi.org/10.1029/2009WR007739>.
- Wörman, A., Wachniew, P., 2007. Reach scale and evaluation methods as limitations for transient storage properties in streams and rivers. *Water Resour. Res.* 43, W10405. <http://dx.doi.org/10.1029/2006WR005808>.
- Zarnetske, J.P., Haggerty, R., Wondzell, S.M., Baker, M.A., 2011. Dynamics of nitrate production and removal as a function of residence time in the hyporheic zone. *J. Geophys. Res.* 116, G01025. <http://dx.doi.org/10.1029/2010JG001356>.